

Private Fuel Storage, L.L.C.

P.O. Box C4010, La Crosse, WI 54602-4010

Phone 303-741-7009 Fax: 303-741-7806

John L. Donnell, P.E., Project Director

Mr. Mark Delligatti
Spent Fuel Project Office
Office of Nuclear Material Safety and Safeguards
U.S. Nuclear Regulatory Commission
Washington, D.C. 20555

March 24, 1999

**SUBMITTAL OF COMMITMENT RESOLUTION INFORMATION
PRIVATE FUEL STORAGE FACILITY
DOCKET NO. 72-22 / TAC NO. L22462
PRIVATE FUEL STORAGE L.L.C.**

Reference: PFSLLC Letter, Donnell to Delligatti, Commitment Resolution,
dated March 17, 1999

Please find enclosed Private Fuel Storage responses to NRC Commitment Resolution
comments (Reference).

If you have any questions regarding this response, please contact me at 303-741-7009.

Sincerely,

John L. Donnell
Project Director
Private Fuel Storage L.L.C.

NIF06/1

Mr. Mark Delligatti

2

March 24, 1999

cc:

John Parkyn

Jay Silberg

Sherwin Turk

Asadul Chowdhury

Murray Wade

Scott Northard

Denise Chancellor

Richard E. Condit

John Paul Kennedy

Joro Walker

John Donnell

ENCLOSURE

1. RAI 4-1 (second round), Thermal Analysis

NRC Comment – The PFSF SAR Section 4.2.1.5.2 and 4.2.2.5.2 identifies a design ambient temperature of 110 F, and RAI 4-1 stated: 'Justify the use of the referenced cask systems at a site where the ambient or off-normal conditions appear to be an unanalyzed temperature condition'. The PFS RAI response did not adequately address the issue.

PFS Response - Based on General Design Criteria 10 CFR 72.122 (b), *protection against environmental conditions and natural phenomena*, systems important to safety must be designed to accommodate and be compatible with site characteristics and environmental conditions. Criteria for the use of a storage system at a storage location are that the conditions set forth by the storage system vendors are met at the storage location.

Both of the PFSF storage systems (Hi-Storm and TranStor) specify criteria for normal conditions as annual average temperatures. The annual average temperature limits for these systems are 80°F for Hi-Storm (Hi-Storm TSAR Section 4.4) and 75°F for TranStor (TranStor SAR Section 4.1). The annual average takes into account both day and night, summer and winter temperatures throughout the year. The annual average temperature is the principal design parameter in the storage system design analyses because it establishes the basis for demonstration of long-term spent nuclear fuel integrity. The long-term integrity of the spent fuel cladding is a function of the averaged ambient temperature over the entire storage period, which is assumed to be at the maximum average yearly temperature in every year of storage for conservatism in the cladding service life computations.

The criteria for off-normal conditions established for both storage systems is based on a 24 hour average solar load based on 10 CFR 71, which represents extreme environmental conditions or off-normal conditions. The maximum off-normal temperature condition for both systems is 100°F (Hi-Storm TSAR Section 11.1.2 and TranStor SAR Section 11.1.1). This off-normal temperature is a 24-hour average solar load subjected to the storage system.

To show that PFSF meets the Hi-Storm and TranStor design criteria, the site design temperatures stated in the PFSF Safety Analysis Report will be revised to be consistent with the vendors' definitions for their temperature limits corresponding to the annual average temperature and an off-normal maximum daily average temperature. The 110°F site design ambient temperature, currently stated in the SAR, will be replaced since it does not relate to the storage system temperature criteria requirements.

ENCLOSURE (con't)

Based on data recorded for areas near the site, Dugway (12 miles South) and Iosepa South Ranch (8 miles NW), and the PFS met tower, the annual average temperature and the highest recorded average daily maximum temperature for July are as follows:

<u>Temperatures, F</u>	<u>Dugway¹</u>	<u>Iosepa Ranch¹</u>	<u>PFSF Met Data²</u>
Annual Average (°F)	51.0	50.0	49.0
Average Daily Maximum (°F)	94	95	92.6

If the highest values are selected for conservatism to represent the PFSF site design temperatures, the annual average temperature is 51 °F and the highest recorded average daily maximum temperature is 95 °F.

The highest 24 hour average temperature, which correlates with the vendor's off-normal temperature of 100 °F, was recorded at the PFSF Met Tower as 83.8 °F and was not available in the data for Dugway and Iosepa. The "average daily maximum temperature," which has been used to date in the RAI thermal discussions regarding off-normal temperatures, is an average of the peak temperatures throughout the hottest month of July. Use of this temperature value, which bounds any 24 hour average, provides an ample margin from the vendor's 100 °F off-normal temperature.

Since the highest annual average temperature of 51 °F is less than the Hi-Storm 80 °F and the TranStor 75 °F and the highest average daily maximum temperature of 95 °F is less than the vendors' 100 °F, no unanalyzed condition exists.

References

1. Ashcroft, G.L., D.T. Jensen and J.L. Brown, 1992, Utah climate: Logan, UT, Utah Climate Center, Utah State University (1950 – 1992 Dugway data and 1951 – 1958 Iosepa South Ranch data).
2. PFSF Meteorological Data taken during 1997 and 1998.

ENCLOSURE (con't)

2. RAI 2-5 (first round), Seismic Analysis

NRC Comment – Some of the equations provided by the Geomatrix report (Sections 6 and 7) in support of the response to RAI 2-5 are not clear with respect to some of the variables used. Also, equations used in conjunction with the Yucca Mountain studies are not clear as to their applicability to the PFSF site.

PFS Response – A clarification of the PSHA formulation is provided as Attachment 1.

ATTACHMENT 1

CLARIFICATION OF PSHA FORMULATION

(Six pages plus Figures C-1, C-2, and C-3)

CLARIFICATION OF PSHA FORMULATION

PSHA Formulation for Ground Motion Hazard

Equation (6-2) of the text, repeated below, is the basic equation used in computing the ground shaking hazard. The hazard is expressed as the frequency of exceeding a specified level of ground motion, $v(z)$, where z is the ground motion level. Given a *known* set of models and model parameters for representing the frequency of earthquake occurrence, the randomness of size and location of future earthquakes, and the randomness in the level of ground motion they may produce at the site, $v(z)$ is computed by the expression:

$$v(z) = \sum_n \alpha_n(m^0) \int_{m^0}^{m''} f(m) \left[\int_0^{\infty} f(r|m) \cdot P(Z > z|m, r) \cdot dr \right] \cdot dm \quad (6-2)$$

where $\alpha_n(m^0)$ is the frequency of all earthquakes on source n above a minimum magnitude of engineering significance, m^0 ; $f(m)$ is the probability density of earthquake size between m^0 and a maximum earthquake the source can produce, m'' ; $f(r|m)$ is the probability density function for distance to an earthquake of magnitude m occurring on source n ; and $P(Z > z|m, r)$ is the probability that, given an earthquake of magnitude m at distance r from the site, the peak ground motion will exceed level z .

However, the models and model parameters of Equation (6-2) are not known with certainty. They depend upon the collective set of scientific judgments and data interpretations documented in the PSHA report. These can be represented by a set of parameters Θ . The elements of Θ include all of the parameters of Equation (6-2), together with the specific interpretations that lead to those parameters. The uncertainty in Θ is characterized using the logic trees shown on Figures 6-3 and 6-5 of the PSHA report. Each end branch at the right hand side of the log tree defines a specific set of input parameters, θ_i that can be used to compute the hazard using Equation (6-2). The result is a frequency of exceeding ground motion level z that is conditional on θ_i , $v(z|\theta_i)$ and Equation (6-2) can be rewritten as:

$$v(z|\theta_i) = \sum_n \alpha_n(m^0|\theta_i) \int_{m^0}^{m''|\theta_i} f(m|\theta_i) \left[\int_0^{\infty} f(r|m, \theta_i) \cdot P(Z > z|m, r, \theta_i) \cdot dr \right] \cdot dm \quad (C-1)$$

The probability that Θ will take on any particular value θ_i is equal to the joint probability of the set of parameters θ_i being the true parameter values. $P(\Theta = \theta_i)$ is obtained by multiplying the probabilities on all of the branches leading to θ_i :

$$P(\Theta = \theta_i) = \prod_k P(\text{branch}_k | \text{branch}_1 \dots \text{branch}_{k-1}) \quad (\text{C-2})$$

where $P(\text{branch}_k | \text{branch}_1 \dots \text{branch}_{k-1})$ is the probability that a specific branch at node k is the correct branch conditional on all of the branches leading to node k represent the correct path through the logic tree.

As a result of computing the hazard for each end branch of the logic tree, a discrete distribution for $v(z | \Theta)$ is obtained. The expected or mean value of $v(z | \Theta)$ is given by:

$$E[v(z | \Theta)] = \sum_i v(z | \theta_i) \cdot P(\Theta = \theta_i) \quad (\text{C-3})$$

and the fractiles of the distribution are obtained by ordering the values of $v(z | \theta_i)$ and computing the sum of $P(\Theta = \theta_i)$ until the desired fractile levels are reached.

PSHA Formulation for Fault Displacement Hazard

The formulation for probabilistic evaluation of the hazard from fault displacement is analogous to that developed for the hazard from ground shaking. The fault displacement PSHA provides the frequency of exceeding a specified level of displacement, $v(d)$, where d is the amount of fault displacement. Equation (7-1) in the PSHA report presents the basic hazard formulation in its simplest terms:

$$v(d) = \lambda_{DE} \cdot P(D > d) \quad (\text{7-1})$$

where λ_{DE} is the frequency of displacement events and $P(D > d)$ is the conditional probability that the displacement in a single event will exceed value d . The exact form of Equation (7-1) used in the calculation depends upon whether the *earthquake approach* or the *displacement approach* is being used.

For the earthquake approach, λ_{DE} is given by Equation (7-3) in the PSHA report:

$$\lambda_{DE} = \sum_{j=1}^n \lambda_j (\text{Events on source } j) \times P_i(\text{Slip}|\text{Event on source } j) \quad (7-3)$$

where $P_i(\text{Slip}|\text{Event on } j)$ is the probability of slip at point i due to an earthquake on source j , given by Equations (7-4) and (7-5) in the PSHA report, and λ_j is the frequency of earthquakes of different sizes and at different locations from Equation (6-2). Thus, using Equations (6-2) and (7-3), Equation (7-1) is recast as:

$$v(d) = \sum_j \alpha_j (m^0) \int_{m^0}^{m^*} f(m) \left[\int_0^{\infty} f(r|m) \cdot P(\text{slip}|m, r, h) \cdot P(D > d|m, r) \cdot dr \right] \cdot dm \quad (C-4)$$

Because both $P_i(\text{Slip}|\text{Event on } j)$ and $P(D > d)$ vary with earthquake magnitude and source-to-site distance, they are included within the magnitude and distance integrals. [Note that for ground motion hazard, the analogous probability, $P_i(\text{Shaking}|\text{Event on } j)$, is equal to 1.0 because it is assumed that every earthquake will produce some level of shaking at a site, though the level may be very small.] As was the case for Equation (6-2), incorporating the uncertainty in the models and parameters leads to the displacement hazard form of Equation (C-1) for the earthquake approach:

$$v(d|\theta_i) = \sum_j \alpha_j (m^0|\theta_i) \int_{m^0}^{m^*|\theta_i} f(m|\theta_i) \left[\int_0^{\infty} f(r|m, \theta_i) \cdot P(\text{slip}|m, r, h, \theta_i) \cdot P(D > d|m, r, \theta_i) \cdot dr \right] \cdot dm \quad (C-5)$$

where again, θ_i represents a specific set of models and model parameters used to compute the hazard.

For the displacement approach using fault slip rate, the formulation is much simpler, with λ_{DE} given by Equation (7-2) in the PSHA report and $P(D > d)$ dependent on the average displacement per event, \bar{D}_E , and the form of the distribution for D/\bar{D}_E . Incorporating uncertainty in the models and parameters leads to displacement hazard form of Equation (C-1) for the displacement approach:

$$v(d|\theta_i) = \frac{SR|\theta_i}{\bar{D}_E|\theta_i} + P\left(D > d \middle| \bar{D}_E, \theta_i\right) \quad (C-6)$$

The mean hazard integrated over the uncertainty in Θ is computed using Equation (C-3).

Probability of Distributed Slip for Earthquake Approach to Fault Displacement Hazard

For the distributed faulting approach, the probability that an earthquake on source j will cause distributed slip on the feature at point i is computed using the logistic regression model of Equation (7-4) in the PSHA report:

$$P_i(\text{Slip} | \text{Event on } j) = \frac{e^{f(m,r)}}{1 + e^{f(m,r)}} \quad (7-4)$$

where $f(m,r)$ is given by Equation (7-5) in the PSHA report

$$f(m,r,h,\tau) = 3.27 + (-8.28 + 0.577m + 0.629h) \cdot \ln(r + 4.14) + 0.611\tau \quad (7-5)$$

in which h is 1.0 if the site lies in the hanging wall of the rupture and 0.0 if the site lies in the foot wall, and τ is a random variate with 0 mean and unit variance that accounts for variability from earthquake to earthquake. When Equation (7-5) is used to compute the probability of distributed slip, the mean value of $P_i(\text{Slip} | \text{Event on } j)$ is found by integrating over the random effect distribution. Figure C-1 shows the variation in the predicted probability of distributed rupture for a magnitude 6.5 earthquake as the random effect τ is varied from -1.22 to $+1.22$, corresponding to a ± 2 standard deviation range for a normal variate which encompasses 95% of the probability mass. Note that the curves shown on Figure C-1 represent a balance between the data with non zero densities of distributed faulting and the larger mass of data with observed zero density of distributed faulting show by the data points at the bottom of the plots.

The general form of Equation (7-5) was developed as part of the seismic hazard assessment for Yucca Mountain (CRWMS M&O, 1998, Appendix H). The relationship preferred by the majority of the experts was:

$$f(m,r,h) = 2.06 + (-4.62 + 0.118m + 0.682h) \cdot \ln(r + 3.32) \quad (C-7)$$

During application of the displacement hazard methodology in a subsequent project for the Los Alamos National Laboratory (Olig and others, 1998) it was suggested that the distributed faulting data may be more scattered than represented by the form of Equation (C-7) and that a *random effects* model might provide a better fit. Hosmer and Lemeshow (1989, page 141) define a goodness of fit statistic, \hat{C} , for logistic regression in the form of a Pearson χ^2 statistic for a table of observed and predicted frequencies. Using this approach, Olig and others (1998) found a goodness of fit statistic, \hat{C} , for Equation (C-7) of 317 with a p -value of 0.00, indicating that the data are more scattered than expected for the model.

The suggested improvement in the model was adding a random effect term, $\gamma\tau_i$, to Equation (C-7) to represent variability from earthquake to earthquake resulting from unknown variables (e.g. Brillinger and Preisler, 1983). Parameter τ_i is a normal variate with 0 mean and unit variance representing a random effect for the i^{th} event, and γ is a parameter estimated from the data that defines the magnitude of this variation. Brillinger and Preisler (1983) present a general approach for estimating the coefficients of a random effects model using maximum likelihood combined with Gaussian quadrature. Applying this method, Olig and others obtained Equation (7-5). The resulting goodness of fit statistic, \hat{C} , was 8.4 with a p -value of 0.68, indicating a large improvement in the model. Thus, it was judged that the use of Equation (7-5) from Olig and others (1998) rather than Equation (C-7) from the Yucca Mountain study was warranted for computing the displacement hazard at the Skull Valley site.

Figure C-2 compares the predicted probabilities of distributed slip obtained using Equation (C-7) to those obtained using Equation (7-5) with the random effect set to zero. The values obtained using Equation (C-7) are much less sensitive to earthquake magnitude. Figure C-3 shows the effect on the computed displacement hazard of using Equation (C-7) instead of (7-5). At a displacement of 1 cm, there is about a factor of two increase in the frequency of exceedance. The difference between the two results decreases as the displacement level increases. The difference between the two results is primarily due to the lower rate of attenuation of the predicted probabilities of distributed slip from Equation (C-7), which results in a greater contribution from events at larger distances. Because of the attenuation in the amount of slip with distance, these events contribute more to the hazard for small displacements than large displacements. The resulting mean hazard curve using Equation (C-7) in the earthquake approach remains

near or below the hazard computed using the preferred displacement approach. Thus, the overall effect on the total hazard is small.

References

- Brillinger, D.R., and Preisler, H.K., 1983, Maximum likelihood estimation in a latent variable problem: *in* Studies in Econometrics, Time Series, and Multivariate Statistics: S. Karlin, T. Amemiya, and L.A. Goodman (eds.), Academic Press, New York, p. 31-65.
- Hosmer, D.I., and Lemeshow, S. 1989, *Applied Logistic Regression*, John Wiley & Sons, New York, 307 p.
- Olig, S., Youngs, R., and Wong, I., 1998, Probabilistic seismic hazard analysis for surface fault displacement at TA-3, Los Alamos National Laboratory: report prepared for Los Alamos National Laboratory, University of California, 7, July.

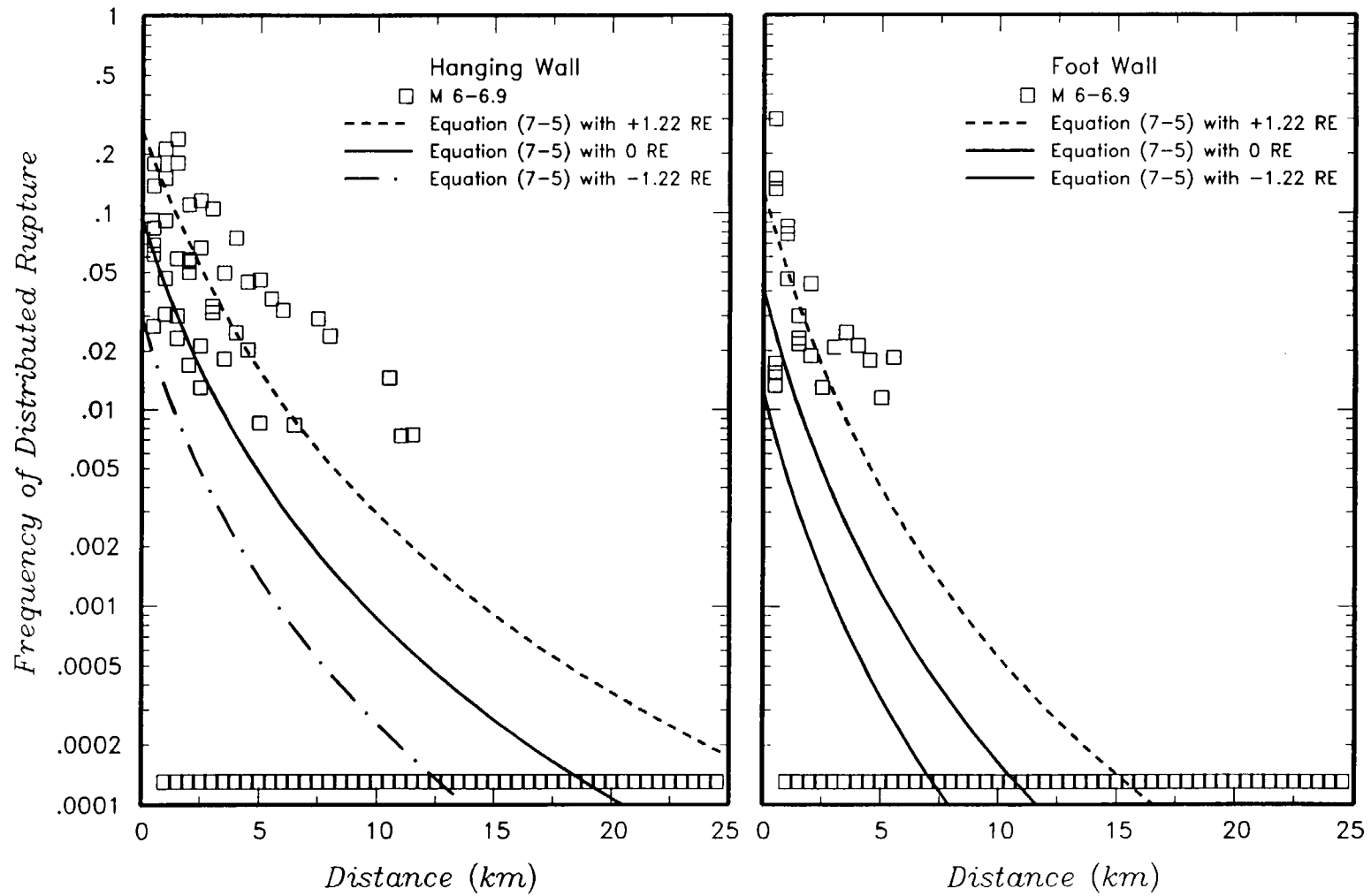


Figure C-1 Range of predicted probability of distributed rupture for magnitude 6.5 earthquakes due to ± 2 standard deviations in the random effect

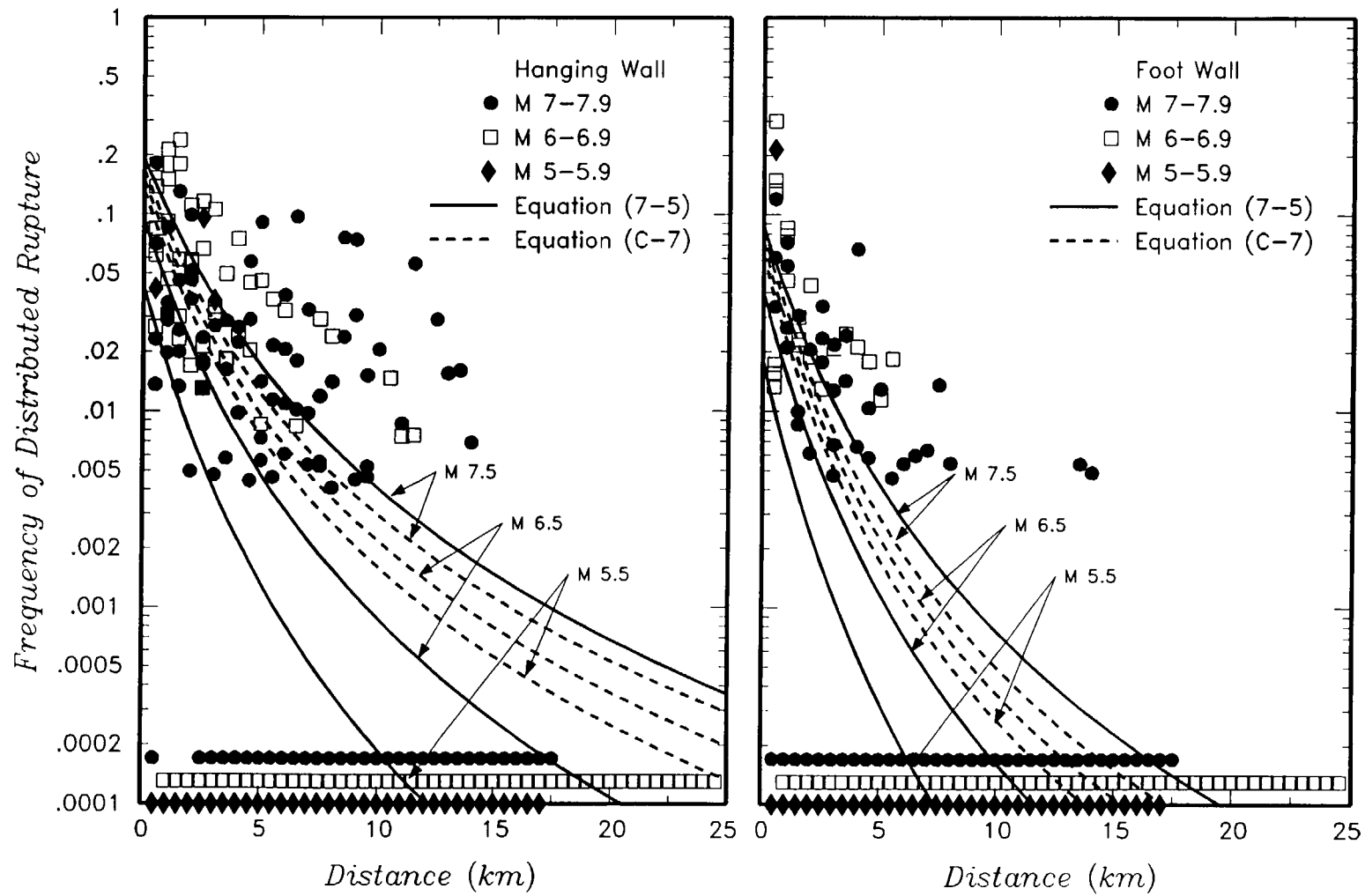


Figure C-2 Comparison of predicted probability of distributed rupture

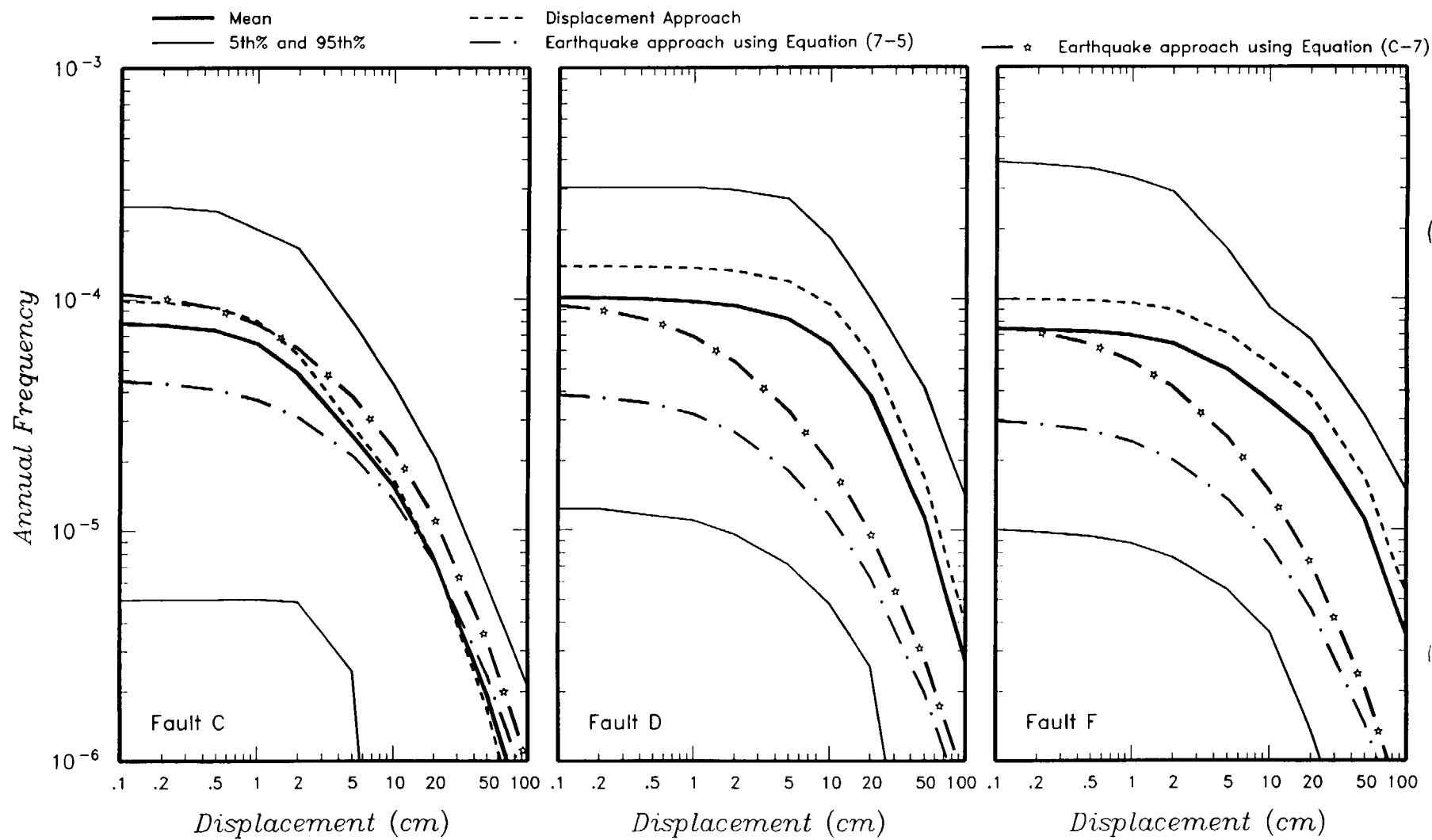


Figure C-3 Comparison of earthquake approach displacement hazard computed using Equation (C-7) with results presented on Figure 7-9 of PSHA report

ENCLOSURE (con't)

3. RAI 8-2 (second round), Onsite Explosion Analysis

NRC Comment – The PFS SAR (Chapter 8) has adequately evaluated the effects of offsite explosions, but not onsite explosions. The PFSF site will have vehicles and a backup generator using diesel fuel with diesel fuel storage tanks, and building heating systems using propane storage tanks that should be considered.

PFS Response

Diesel Fuel Oil Storage Tanks

A diesel fuel oil storage tank will be located inside the restricted area (RA), and will supply diesel fuel oil for onsite vehicles, including the cask transporter. This tank will be located near the RA fence, approximately 200 ft northeast of the northeast corner of the Canister Transfer Building and approximately 700 ft from the nearest storage casks. A double-wall subbase diesel fuel oil tank will be mounted on the backup diesel generator skid in the Security and Health Physics Building to provide fuel for operation of the backup diesel generator. This area will be protected with a fire suppression system designed to NFPA 13 requirements for water sprinklers. A fire involving the indoor tank will not affect structures, systems or components outside of the Security and Health Physics Building. The outdoor tank will be above-ground, and will be designed in accordance with the requirements of NFPA 30, with dikes around the tank to contain fuel in the event of leaks or spillage.

While unlikely, it is considered possible that collision or tornado-driven missile impact with the outdoor tank could result in tank rupture and spillage of diesel fuel oil. If there were an ignition source at the location of the spilled diesel fuel, it would be possible to initiate a fire, though diesel fuel is difficult to ignite due to its low volatility. Rupture of a storage tank and spillage of diesel fuel does not create the potential for an explosion. It is planned to use Grade Low Sulfur No. 2-D diesel fuel oil in both applications (onsite vehicles and backup diesel generator), which has a flash point of 126F (52C) per Reference 1. Diesel fuel is not a flammable liquid (defined as a liquid having a flash point below 100F), but falls into the classification of a Class II combustible liquid which has a flash point above 100F and below 140F (Reference 2). The flash point is defined as the lowest temperature at which the vapor pressure of the liquid is just sufficient to produce a flammable mixture at the lower limit of flammability above the surface of the liquid. In recognition of the relatively high flash point of diesel fuel oil (at above-ambient temperatures), NFPA 30 does not require use of explosion proof electrical equipment in the vicinity of diesel fuel oil. While spilled diesel fuel could burn it could not detonate, and therefore an explosion associated with diesel fuel oil is not considered to be a credible event. The outdoor diesel fuel oil storage tank is sufficiently removed from the Canister Transfer Building and the storage casks (nearest important-to-safety structures, systems, and components) that radiant heat energy from a diesel fuel oil fire at the storage tank would not result in damage.

ENCLOSURE (con't)

Propane Fuel Storage Tanks

Propane for heating the Canister Transfer Building and the Security and Health Physics Building is stored in two 1,000 gallon propane fuel storage tanks, located outside of the RA, approximately 400 ft east of the Canister Transfer Building and 1,030 ft from the nearest storage casks. The storage tanks will be above-ground, designed in accordance with the requirements of NFPA 58. Propane is stored as a liquefied petroleum gas with the tank pressurized to the vapor pressure of the propane liquid, whose temperature will be close to the average ambient daily temperature. The vapor pressure of commercial propane is 132 psig at 70F and 216 psig at 105F (Table 5-5E of Reference 2). Relief valves on the tank will be set at approximately 275 psig. Propane is classified as a flammable liquid, and at standard atmospheric pressure (14.7 psia) commercial propane has a boiling point of minus 51F (Table 5-5E of Reference 2). It is heavier than air, with propane vapor having a specific gravity of 1.52 at 60F (Table 5-5E of Reference 2, with specific gravity air = 1). NFPA 58 requires that propane tanks between 50 and 2,000 gallon capacity be located at least 25 ft away from any building, adjacent container, or adjacent property.

At 60F, one gallon of propane liquid weighs 4.24 lbs (Table 5-5E of Reference 2). It is conservatively assumed that one of the propane tanks contains 1,000 gallons of liquefied propane and that it ruptures. The total weight of propane is (1,000 gal) (4.24 lb/gal) = 4,240 lbs. It is also conservatively assumed that a large fraction of this propane mixes with air so that it is in an explosive concentration (in range of 2.15% to 9.60%, per Table 5-5E of Reference 2), ignites, and is involved in an explosion. The magnitude of the postulated explosion can be assessed using the TNT energy equivalent methodology discussed in Reg. Guide 1.91 (Reference 3). This Reg. Guide states the following:

"Application of the TNT equivalence concept to possible detonations of vapor clouds formed after an accidental release of hydrocarbons is not as well documented. However, investigations of accidents that resulted in blast damage have used this concept in attempts to estimate, based on blast damage, the effective yield of the explosion (Ref. 3). Most assessments of this type have led to estimates that less than one percent of the calorific energy of the substance was released in blast effects. Since the ratios of heat of combustion of hydrocarbons to that of TNT are typically about 10, this corresponds to an equivalence on a mass basis of 10 percent. The blast energy realized depends, in great measure, on phenomena that are accident specific, i.e., the rate of release of the substance and the way in which the cloud is ignited. A reasonable upper bound to the blast energy potentially available based on experimental detonations of confined vapor clouds is a mass equivalence of 240 percent (Ref. 4). A detailed analysis of possible accident scenarios for particular sites, including consideration of the actual cargo, site topography, and prevailing meteorological conditions may justify a lower effective yield. But, when establishing safe stand-off distances independent of site conditions, use of an upper bound is prudent."

ENCLOSURE (con't)

It is considered that use of the 240 percent equivalence is overly conservative for this application, since the propane/air mixture will not be confined. The propane tanks will be in the open, with no structures around them. The TNT energy equivalence of 4,240 lbs of propane is estimated as follows:

Based on Table 5-5E of Reference 2, the total heating value of commercial propane after vaporization is 21,591 Btu/lb. 4,240 lbs of propane has a total heating value of 9.155 E7 Btu, equal to 2.31 E10 calories. Reference 3 indicates that investigations led to estimates that less than one percent of the calorific energy of hydrocarbon gas/air vapor clouds that exploded was released in blast effects. It is conservatively assumed that 25% of the vapor is in a flammable gas-air mixture having concentrations ranging from the lower flammable limit of 2.15% to the upper flammable limit of 9.60% (Table 5-5E of Reference 2) and that 10% of the total heat of combustion of this flammable mixture is released in blast effects.

$$\text{Energy Released in Blast} = (2.31 \text{ E}10 \text{ cal}) (0.25) (0.10) = 5.78 \text{ E}8 \text{ cal.}$$

Trinitrotoluene (TNT) has a "heat of explosion" of 1,050 cal/g (Reference 4). The equivalent weight of TNT that would release 5.78 E8 calories of heat energy is:

$$(5.78 \text{ E}8 \text{ calories} / (1.05 \text{ E}3 \text{ cal/g}) = 5.505 \text{ E}5 \text{ g} = 1.214 \text{ lbs}$$

The overpressure effects of postulated detonation of this weight of TNT can be assessed using Figure 4-12 of Reference 5, "Shock-Wave Parameters for Hemispherical TNT Surface Explosion at Sea Level". This Reference 5 Army Technical Manual on Explosion Effects is Ref. 1 of Reg. Guide 1.91, and provides the basis for Figure 1 of the Reg Guide. Figure 4-12 of Reference 5 presents overpressures at various scaled ground distances from TNT detonations, with varying weights of TNT.

$$\text{The scaled ground distance, } Z_G = R_G / W^{1/3}$$

$$\text{where } W^{1/3} = (1,214)^{1/3} = 10.67$$

While the storage casks can withstand a much higher overpressure before they begin to slide or tip, the Canister Storage Building is designed to withstand a pressure differential of 1.5 psi due to a tornado (PFSF SAR Sections 3.2.8.1 and 3.2.8.3) and an even higher load due to a seismic event. Therefore, the limiting overpressure for important-to-safety structures that could be impacted by a propane explosion is considered to be 1.5 psi. A 1.5 psi peak positive incident pressure corresponds to a scaled ground distance, Z_G , of approximately 32, as scaled from Figure 4-12 of Reference 5. Solving the above equation for R_G :

ENCLOSURE (con't)

$$Z_G = R_G / W^{1/3}, 32 = R_G / 10.67, R_G = (32)(10.67) = 341 \text{ ft}$$

Thus, based on the TNT energy equivalence approach and Reference 5, the resulting overpressure from a propane explosion will not exceed 1.5 psi at important-to-safety structures as long as the propane tank is located a distance of at least 341 ft from the Canister Transfer Building and storage casks. The propane tanks will be sited east of the Canister Transfer Building, at a distance of approximately 400 ft, which locates them approximately 1,030 ft from the nearest storage casks. This assures that postulated explosion of propane leaked from a tank will not produce overpressures greater than 1.5 psi and will not challenge the integrity of the storage casks or the Canister Transfer Building.

References

1. American Society for Testing and Materials (ASTM) Standard D975-1997, Standard Specification for Diesel Fuel Oils.
2. Fire Protection Handbook, Sixteenth Edition, National Fire Protection Association, 1986.
3. U.S. NRC Regulatory Guide 1.91, "Evaluations of Explosions Postulated to Occur on Transportation Routes near Nuclear Power Plants", Rev. 1, February 1978; for comment).
4. Rudolph Meyer, "Explosives", 3rd Edition, 1987.
5. Department of the Army Technical Manual TM 5-1300, "Structures to Resist the Effects of Accidental Explosions," June 1969.

4. RAI's 2-1 & 2-2 (second round), Geotechnical Program

NRC Comment – The PFS field geotechnical investigation program is limited in the number of borings and tests provided. PFS should perform an evaluation of the Standard Penetration Test blow counts (N-values), individually, rather than averaged over 5-ft intervals, to demonstrate that the variability in N-values across the site is not significant. Atterberg Limits, shear strength, and compressibility should also be addressed.

PFS Response – PFS reviewed the variability of N-values across the site, evaluating the Standard Penetration Test (SPT) blow counts individually, rather than averaged over 5-ft intervals, and reports the findings below.

Tables 1, 2, and 3 present matrices of the N-values vs depth for all of the borings drilled in the proposed emplacement area. In these matrices, the borings are arranged to correspond with their locations in the field, with north situated at the top of the sheet. For example, Boring A-1, which was drilled in the northwest corner of the proposed emplacement area, is located in the upper left corner of the matrix. Borings B-1, C-1, and D-1 were drilled in locations east of A-1, and these are arranged to the right of A-1 in the matrix. Boring A-2 was drilled at a location south of A-1, and it is arranged in the matrix in the row just below A-1. The remaining borings are located similarly with respect to their locations in the plan view. This results, therefore, in Borings A-4 through D-4 being located at the bottom of the matrix, with A-4 on the left (i.e., the southwestern corner of the proposed emplacement area) and D-4 on the far right (i.e., the southeastern corner of the proposed emplacement area).

In order to evaluate the variability of the blow count data, the low blow counts, arbitrarily defined as N-values less than 10 blows/ft, are highlighted by gray shading in Tables 1 and 2, and blow counts in the range from 10 to 15 blows/ft are highlighted in Table 3. Table 1 includes all of the SPT data, whereas Tables 2 and 3 exclude Samples S-1, which were obtained at a depth of 0 to 1.5 ft in each of the borings. These shallow samples represent soils that will be removed before constructing the cask storage pads; therefore, their blow counts are not pertinent to the design of these foundations.

These matrices illustrate that the soils in the upper layer of the profile do not vary significantly across the site based on their SPT blow counts. Table 2 illustrates that there generally is one or two SPT samples in each of the borings with N-values less than 10 blows/ft. Table 3 also illustrates at a glance that the N-values within the range of 10 to 15 blows/ft are even less variable across the site than are the lower blow counts. Therefore, it is concluded that the SPT blow count data do demonstrate that the soils in the upper layer are uniform across the site and there is not sufficient variability in the blow counts to justify requiring individual design parameters for each pad.

ENCLOSURE (con't)

A quick glance at Table 2 might lead one to conclude that conditions at the north and west are different than elsewhere on site because there are no highlighted low blow counts in Borings A-1, B-1, and A-2. However, undisturbed tubes U-2, which were obtained at a depth of 6 to 8 ft in Borings B-1 and A-2 would likely have had N-values less than 10 if the SPT test had been performed instead of taking undisturbed samples at these locations. More significant, however, is the fact that the lack of low blow counts in this area, as well as in the northeast (Boring D-1) and the southwest (Boring A-4), indicates that the soils would perform better than those that were tested. Three of the consolidation tests were performed on Sample U-3 in Boring C-1, which was obtained just below a low blow sample. One of the consolidation tests and one of the UU tests were performed on Sample U-2 in Boring C-2, which was surrounded by borings with low blow counts (Borings B-2, C-1, D-2, and C-3). The remaining UU test was performed on Sample U-3 in Boring B-4, which also was obtained just below a low blow count sample. Therefore, the samples that were tested for strength and compressibility were representative of the lower blow count soils and, thus, extrapolating the results of those tests to the other soils within the upper layer that had higher blow counts should provide conservative estimates of the strength and compressibility for those soils.

Additional field work, recently performed at the site, is described in Geomatrix Consultants, Inc., Final Report Fault Evaluation Study and Seismic Hazard Assessment, February 1999 and included detailed lithostratigraphic soils mapping in test pits and trenches, as well as logging of continuous split-barrel samples in closely spaced boreholes. The results of these studies reaffirm the uniformity of the upper layer of the subsurface profile at the PFSF.

Subsurface profiles and stratigraphic descriptions are presented in Plates 3 and 4 in Geomatrix report, and they illustrate convincingly that the subsurface conditions are very uniform. They identify a thin (<2.5 ft) surface layer of eolian silt and playa deposits with a poorly developed soil structure. This layer corresponds to the first SPT sample in the SWEC borings that were drilled in late 1996 (SAR Appendix 2A) in the proposed emplacement area. This layer is underlain by a sequence of typical lacustrine sediments associated with several stages of Lake Bonneville, an inland sea that covered the area from about 30,000 to 10,000 years before present (B.P.). These sediments are, by and large, the fine-grained end members of a ternary diagram consisting of silt, clay, and sand. Samples are consistently described as silt, silty clay, clayey silt, or sandy silt. Geomatrix used the term marl or marly as an additional component of these descriptions, which refers to a high calcium carbonate content clay or silt deposited in a fresh-water environment (deep-water facies of Bonneville alloformation).

Geomatrix was able to subdivide the lacustrine sequence into several lake stages based on sedimentary relationships and physical characteristics exposed in continuous wall exposures in trenches and test pits. Their subdivisions of the Bonneville

— ENCLOSURE (con't) —

alloformation, presented in their Plate 3, "Map of North Wall Trench T-2", are as follows:

Bonneville Deep-Water Blocky,
Bonneville Deep-Water Laminated,
Post-Stansbury Transgressive, and
Stansbury Regressive.

This sequence extends to a depth of about 25 to 30 ft, where a continuous, nearly horizontal layer of dense, fine sand is encountered. This layer is the "Stansbury Transgressive", and it represents the oldest deposit of the Bonneville Cycle. The base of this unit occurs at a depth of about 45 to 50 ft and is believed to be an unconformity represented by the Promontory soil. This boundary is an apparent seismic velocity contrast that is recognizable on the recent seismic reflection profiles as a continuous, nearly horizontal layer, the Qp reflector (Geomatrix Consultants, Inc, 1999).

TABLE 1
MATRIX OF SPT BLOW COUNT DATA IN PROPOSED EMPLACEMENT AREA
N < 10 BLOWS/FT FOR ALL SAMPLES

ID	Sample	z_{avg}	N	ID	Sample	z_{avg}	N	ID	Sample	z_{avg}	N	ID	Sample	z_{avg}	N
A-1	S 1	0.8	23	B-1	S 1	0.8	13	C-1	S 1	0.8	3	D-1	S 1	0.8	40
A-1	S 2	5.8	13	B-1	U 2	6.0	TUBE	C-1	S 2	5.8	8	D-1	S 2	5.8	12
A-1	S 3	10.8	22	B-1	S 3	10.8	15	C-1	U 3	11.0	TUBE	D-1	S 3	10.8	14
A-1	S 4	15.8	19	B-1	S 4	15.8	20	C-1	S 4	15.8	16	D-1	S 4	15.8	13
A-1	S 5	20.8	13	B-1	S 5	20.8	12	C-1	S 5	20.8	8	D-1	S 5	20.8	16
A-1	S 6	25.8	36	B-1	S 6	25.8	45	C-1	S 6	25.8	60	D-1	S 6	25.8	100
A-1	S 7	30.8	149	B-1	S 7	30.8	70	C-1	S 7	30.8	91	D-1	S 7	30.8	90
A-1	S 8	35.8	114	B-1	S 8	35.8	90	C-1	S 8	35.8	45	D-1	S 8	35.8	75
A-1	S 9	40.8	70	B-1	S 9	40.8	33	C-1	S 9	40.8	115	D-1	S 9	40.8	100
A-1	S 10	45.8	80	B-1	S 10	45.8	63	C-1	S 10	45.8	85	D-1	S 10	45.8	110
A-1	S 11	50.8	120	B-1	S 11	50.8	125	C-1	S 11	50.8	110	D-1	S 11	50.8	138
A-1	S 12	55.8	110												
A-1	S 13	60.8	102												
A-1	S 14	65.8	54												
A-1	S 15	67.0	100/6"												
A-1	S 16	70.8	100+												
A-1	S 17	75.5	100/6"												
A-1	S 18	80.2	100/4"												
A-1	S 19	85.2	100/4"												
A-1	S 20	90.5	100/6"												
A-1	S 21	95.3	100/6"												
A-1	S 22	100.5	100/6"												

A-2	S 1	0.8	1	B-2	S 1	0.8	4	C-2	S 1	0.8	18	D-2	S 1	0.8	6
A-2	U 2	6.0	TUBE	B-2	S 2	5.8	5	C-2	U 1	6.0	TUBE	D-2	S 2	5.8	6
A-2	S 3	10.8	11	B-2	U 1	9.0	TUBE	C-2	U 2	11.0	TUBE	D-2	S 3	10.8	11
A-2	S 4	15.8	14	B-2	S 3	10.8	13	C-2	S 2	15.8	13	D-2	S 4	15.8	15
A-2	S 5	20.8	17	B-2	S 4	15.8	16	C-2	S 3	20.8	11	D-2	S 5	20.8	18
A-2	S 6	25.8	16	B-2	S 5	20.8	12	C-2	S 4	25.8	34	D-2	S 6	25.8	17
A-2	S 7	30.8	51	B-2	S 6	25.8	15	C-2	S 5	30.8	187/8"	D-2	S 7	30.8	107
A-2	S 8	35.8	175/11"	B-2	S 7	30.8	71	C-2	S 6	35.8	128	D-2	S 8	35.8	121
A-2	S 9	40.4	100/4"	B-2	S 8	35.8	171/11"	C-2	S 7	40.8	181/11"	D-2	S 9	40.8	105
A-2	S 10	45.8	105	B-2	S 9	40.8	68	C-2	S 8	45.8	84	D-2	S 10	45.8	80
A-2	S 11	50.5	100/6"	B-2	S 10	45.8	100/5"	C-2	S 9	50.8	120	D-2	S 11	50.8	150
				B-2	S 11	50.5	100/6"								

A-3	S 1	0.8	4	B-3	S 1	0.8	9	C-3	S 1	0.8	11	D-3	S 1	0.8	6
A-3	S 2	5.8	9	B-3	U 1	6.0	TUBE	C-3	S 2	5.8	6	D-3	S 2	5.8	14
A-3	S 3	10.8	15	B-3	U 2	11.0	TUBE	C-3	S 3	10.8	8	D-3	S 3	10.8	11
A-3	S 4	15.8	15	B-3	S 2	15.8	18	C-3	S 4	15.8	10	D-3	S 4	15.8	9
A-3	S 5	20.8	20	B-3	S 3	20.8	12	C-3	S 5	20.8	9	D-3	S 5	20.8	11
A-3	S 6	25.8	30	B-3	S 4	25.8	24	C-3	S 6	25.8	22	D-3	S 6	25.8	39
A-3	S 7	30.8	34	B-3	S 5	30.8	28	C-3	S 7	30.8	135	D-3	S 7	30.8	100/4"
A-3	S 8	35.8	114	B-3	S 6	35.8	141	C-3	S 8	35.5	100/6"	D-3	S 8	35.3	100/5"
A-3	S 9	40.8	175	B-3	S 7	40.8	150	C-3	S 9	40.8	94	D-3	S 9	40.5	100/5"
A-3	S 10	45.8	82	B-3	S 8	45.8	52	C-3	S 10	45.8	143/11"	D-3	S 10	45.5	100/4"
A-3	S 11	50.5	100/5"	B-3	S 9	50.8	115	C-3	S 11	50.5	100/5"	D-3	S 11	50.8	75/6"

A-4	S 1	0.8	14	B-4	S 1	0.8	22	C-4	S 1	0.8	15	D-4	S 1	0.8	8
A-4	S 2	5.8	18	B-4	S 2	5.8	9	C-4	S 2	5.8	7	D-4	S 2	5.8	4
A-4	S 3	10.8	13	B-4	U 3	11.0	TUBE	C-4	S 3	10.8	11	D-4	S 3	10.8	24
A-4	S 4	15.8	18	B-4	S 4	15.8	15	C-4	S 4	15.8	14	D-4	S 4	15.8	22
A-4	S 5	20.8	12	B-4	S 5	20.8	21	C-4	S 5	20.8	15	D-4	S 5	20.8	9
A-4	S 6	25.8	20	B-4	S 6	25.8	21	C-4	S 6	25.8	20	D-4	S 6	25.8	16
A-4	S 7	30.8	50	B-4	S 7	30.8	34	C-4	S 7	30.8	21	D-4	S 7	30.8	65
A-4	S 8	35.8	93	B-4	S 8	35.8	41	C-4	S 8	35.8	80	D-4	S 8	35.8	88
				B-4	S 9	40.8	95	C-4	S 9	40.8	150	D-4	S 9	40.8	67
				B-4	S 10	45.8	100	C-4	S 10	45.8	70	D-4	S 10	45.8	83
				B-4	S 11	50.8	135	C-4	S 11	50.8	135/11"	D-4	S 11	50.8	160
												D-4	S 12	55.8	132
												D-4	S 13	60.8	45
												D-4	S 14	65.8	100
												D-4	S 15	70.4	100/3"
												D-4	S 16	75.4	100/2"
												D-4	S 17	80.3	50/0"
												D-4	S 18	85.4	100/3"
												D-4	S 19	90.1	100/4"
												D-4	S 20	95.6	170/9"
												D-4	S 21	100.3	50/0"

TABLE 1

TABLE 2
MATRIX OF SPT BLOW COUNT DATA IN PROPOSED EMPLACEMENT AREA
N < 10 BLOWS/FT BELOW A DEPTH OF 1.5 FT

ID	Sample	z_{avg}	N	ID	Sample	z_{avg}	N	ID	Sample	z_{avg}	N	ID	Sample	z_{avg}	N
A-1	S 2	5.8	13	B-1	U 2	6.0	TUBE	C-1	S 2	5.8	6	D-1	S 2	5.8	12
A-1	S 3	10.8	22	B-1	S 3	10.8	15	C-1	U 3	11.0	TUBE	D-1	S 3	10.8	14
A-1	S 4	15.8	19	B-1	S 4	15.8	20	C-1	S 4	15.8	16	D-1	S 4	15.8	13
A-1	S 5	20.8	13	B-1	S 5	20.8	12	C-1	S 5	20.8	8	D-1	S 5	20.8	16
A-1	S 6	25.8	36	B-1	S 6	25.8	45	C-1	S 6	25.8	60	D-1	S 6	25.8	100
A-1	S 7	30.8	149	B-1	S 7	30.8	70	C-1	S 7	30.8	91	D-1	S 7	30.8	90
A-1	S 8	35.8	114	B-1	S 8	35.8	90	C-1	S 8	35.8	45	D-1	S 8	35.8	75
A-1	S 9	40.8	70	B-1	S 9	40.8	33	C-1	S 9	40.8	115	D-1	S 9	40.8	100
A-1	S 10	45.8	80	B-1	S 10	45.8	63	C-1	S 10	45.8	85	D-1	S 10	45.8	110
A-1	S 11	50.8	120	B-1	S 11	50.8	125	C-1	S 11	50.8	110	D-1	S 11	50.8	138
A-1	S 12	55.8	110												
A-1	S 13	60.8	102												
A-1	S 14	65.8	54												
A-1	S 15	67.0	100/6"												
A-1	S 16	70.8	100+												
A-1	S 17	75.5	100/6"												
A-1	S 18	80.2	100/4"												
A-1	S 19	85.2	100/4"												
A-1	S 20	90.5	100/6"												
A-1	S 21	95.3	100/6"												
A-1	S 22	100.5	100/6"												

A-2	U 2	6.0	TUBE	B-2	S 2	5.8	9	C-2	U 1	6.0	TUBE	D-2	S 2	5.8	6
A-2	S 3	10.8	11	B-2	U 1	9.0	TUBE	C-2	U 2	11.0	TUBE	D-2	S 3	10.8	11
A-2	S 4	15.8	14	B-2	S 3	10.8	13	C-2	S 2	15.8	13	D-2	S 4	15.8	15
A-2	S 5	20.8	17	B-2	S 4	15.8	16	C-2	S 3	20.8	11	D-2	S 5	20.8	18
A-2	S 6	25.8	16	B-2	S 5	20.8	12	C-2	S 4	25.8	34	D-2	S 6	25.8	17
A-2	S 7	30.8	51	B-2	S 6	25.8	15	C-2	S 5	30.8	187/8"	D-2	S 7	30.8	107
A-2	S 8	35.8	175/11"	B-2	S 7	30.8	71	C-2	S 6	35.8	128	D-2	S 8	35.8	121
A-2	S 9	40.4	100/4"	B-2	S 8	35.8	171/11"	C-2	S 7	40.8	181/11"	D-2	S 9	40.8	105
A-2	S 10	45.8	105	B-2	S 9	40.8	68	C-2	S 8	45.8	84	D-2	S 10	45.8	80
A-2	S 11	50.5	100/6"	B-2	S 10	45.8	100/5"	C-2	S 9	50.8	120	D-2	S 11	50.8	150
				B-2	S 11	50.5	100/6"								

A-3	S 2	5.8	9	B-3	U 1	6.0	TUBE	C-3	S 2	5.8	6	D-3	S 2	5.8	14
A-3	S 3	10.8	15	B-3	U 2	11.0	TUBE	C-3	S 3	10.8	8	D-3	S 3	10.8	11
A-3	S 4	15.8	15	B-3	S 2	15.8	18	C-3	S 4	15.8	10	D-3	S 4	15.8	9
A-3	S 5	20.8	20	B-3	S 3	20.8	12	C-3	S 5	20.8	9	D-3	S 5	20.8	11
A-3	S 6	25.8	30	B-3	S 4	25.8	24	C-3	S 6	25.8	22	D-3	S 6	25.8	39
A-3	S 7	30.8	34	B-3	S 5	30.8	28	C-3	S 7	30.8	135	D-3	S 7	30.8	100/4"
A-3	S 8	35.8	114	B-3	S 6	35.8	141	C-3	S 8	35.5	100/6"	D-3	S 8	35.3	100/5"
A-3	S 9	40.8	175	B-3	S 7	40.8	150	C-3	S 9	40.8	94	D-3	S 9	40.5	100/5"
A-3	S 10	45.8	82	B-3	S 8	45.8	52	C-3	S 10	45.8	143/11"	D-3	S 10	45.5	100/4"
A-3	S 11	50.5	100/5"	B-3	S 9	50.8	115	C-3	S 11	50.5	100/5"	D-3	S 11	50.8	75/6"

A-4	S 2	5.8	18	B-4	S 2	5.8	9	C-4	S 2	5.8	7	D-4	S 2	5.8	4
A-4	S 3	10.8	13	B-4	U 3	11.0	TUBE	C-4	S 3	10.8	11	D-4	S 3	10.8	24
A-4	S 4	15.8	18	B-4	S 4	15.8	15	C-4	S 4	15.8	14	D-4	S 4	15.8	22
A-4	S 5	20.8	12	B-4	S 5	20.8	21	C-4	S 5	20.8	15	D-4	S 5	20.8	9
A-4	S 6	25.8	20	B-4	S 6	25.8	21	C-4	S 6	25.8	20	D-4	S 6	25.8	16
A-4	S 7	30.8	50	B-4	S 7	30.8	34	C-4	S 7	30.8	21	D-4	S 7	30.8	65
A-4	S 8	35.8	93	B-4	S 8	35.8	41	C-4	S 8	35.8	80	D-4	S 8	35.8	88
				B-4	S 9	40.8	95	C-4	S 9	40.8	150	D-4	S 9	40.8	67
				B-4	S 10	45.8	100	C-4	S 10	45.8	70	D-4	S 10	45.8	83
				B-4	S 11	50.8	135	C-4	S 11	50.8	135/11"	D-4	S 11	50.8	160
												D-4	S 12	55.8	132
												D-4	S 13	60.8	45
												D-4	S 14	65.8	100
												D-4	S 15	70.4	100/3"
												D-4	S 16	75.4	100/2"
												D-4	S 17	80.3	50/0"
												D-4	S 18	85.4	100/3"
												D-4	S 19	90.1	100/4"
												D-4	S 20	95.6	170/9"
												D-4	S 21	100.3	50/0"

TABLE 2

TABLE 3
MATRIX OF SPT BLOW COUNT DATA IN PROPOSED EMPLACEMENT AREA
10 < N < 15 BLOWS/FT BELOW A DEPTH OF 1.5 FEET

ID	Sample	z_{avg}	N	ID	Sample	z_{avg}	N	ID	Sample	z_{avg}	N	ID	Sample	z_{avg}	N
A-1	S 2	5.8	13	B-1	U 2	6.0	TUBE	C-1	S 2	5.8	8	D-1	S 2	5.8	12
A-1	S 3	10.8	22	B-1	S 3	10.8	15	C-1	U 3	11.0	TUBE	D-1	S 3	10.8	14
A-1	S 4	15.8	19	B-1	S 4	15.8	20	C-1	S 4	15.8	16	D-1	S 4	15.8	13
A-1	S 5	20.8	13	B-1	S 5	20.8	12	C-1	S 5	20.8	8	D-1	S 5	20.8	16
A-1	S 6	25.8	36	B-1	S 6	25.8	45	C-1	S 6	25.8	60	D-1	S 6	25.8	100
A-1	S 7	30.8	149	B-1	S 7	30.8	70	C-1	S 7	30.8	91	D-1	S 7	30.8	90
A-1	S 8	35.8	114	B-1	S 8	35.8	90	C-1	S 8	35.8	45	D-1	S 8	35.8	75
A-1	S 9	40.8	70	B-1	S 9	40.8	33	C-1	S 9	40.8	115	D-1	S 9	40.8	100
A-1	S 10	45.8	80	B-1	S 10	45.8	63	C-1	S 10	45.8	85	D-1	S 10	45.8	110
A-1	S 11	50.8	120	B-1	S 11	50.8	125	C-1	S 11	50.8	110	D-1	S 11	50.8	138
A-1	S 12	55.8	110												
A-1	S 13	60.8	102												
A-1	S 14	65.8	54												
A-1	S 15	67.0	100/6"												
A-1	S 16	70.8	100+												
A-1	S 17	75.5	100/6"												
A-1	S 18	80.2	100/4"												
A-1	S 19	85.2	100/4"												
A-1	S 20	90.5	100/6"												
A-1	S 21	95.3	100/6"												
A-1	S 22	100.5	100/6"												

A-2	U 2	6.0	TUBE	B-2	S 2	5.8	5	C-2	U 1	6.0	TUBE	D-2	S 2	5.8	6
A-2	S 3	10.8	11	B-2	U 1	9.0	TUBE	C-2	U 2	11.0	TUBE	D-2	S 3	10.8	11
A-2	S 4	15.8	14	B-2	S 3	10.8	13	C-2	S 2	15.8	13	D-2	S 4	15.8	15
A-2	S 5	20.8	17	B-2	S 4	15.8	16	C-2	S 3	20.8	11	D-2	S 5	20.8	18
A-2	S 6	25.8	16	B-2	S 5	20.8	17	C-2	S 4	25.8	34	D-2	S 6	25.8	17
A-2	S 7	30.8	51	B-2	S 6	25.8	71	C-2	S 5	30.8	187/8"	D-2	S 7	30.8	107
A-2	S 8	35.8	175/11"	B-2	S 7	30.8	71	C-2	S 6	35.8	128	D-2	S 8	35.8	121
A-2	S 9	40.4	100/4"	B-2	S 8	35.8	171/11"	C-2	S 7	40.8	181/11"	D-2	S 9	40.8	105
A-2	S 10	45.8	105	B-2	S 9	40.8	68	C-2	S 8	45.8	84	D-2	S 10	45.8	80
A-2	S 11	50.5	100/6"	B-2	S 10	45.8	100/5"	C-2	S 9	50.8	120	D-2	S 11	50.8	150
				B-2	S 11	50.5	100/6"								

A-3	S 2	5.8	9	B-3	U 1	6.0	TUBE	C-3	S 2	5.8	6	D-3	S 2	5.8	14
A-3	S 3	10.8	15	B-3	U 2	11.0	TUBE	C-3	S 3	10.8	8	D-3	S 3	10.8	11
A-3	S 4	15.8	15	B-3	S 2	15.8	18	C-3	S 4	15.8	10	D-3	S 4	15.8	9
A-3	S 5	20.8	20	B-3	S 3	20.8	18	C-3	S 5	20.8	9	D-3	S 5	20.8	11
A-3	S 6	25.8	30	B-3	S 4	25.8	24	C-3	S 6	25.8	22	D-3	S 6	25.8	39
A-3	S 7	30.8	34	B-3	S 5	30.8	28	C-3	S 7	30.8	135	D-3	S 7	30.8	100/4"
A-3	S 8	35.8	114	B-3	S 6	35.8	141	C-3	S 8	35.5	100/6"	D-3	S 8	35.3	100/5"
A-3	S 9	40.8	175	B-3	S 7	40.8	150	C-3	S 9	40.8	94	D-3	S 9	40.5	100/5"
A-3	S 10	45.8	82	B-3	S 8	45.8	52	C-3	S 10	45.8	143/11"	D-3	S 10	45.5	100/4"
A-3	S 11	50.5	100/5"	B-3	S 9	50.8	115	C-3	S 11	50.5	100/5"	D-3	S 11	50.8	75/6"

A-4	S 2	5.8	18	B-4	S 2	5.8	9	C-4	S 2	5.8	7	D-4	S 2	5.8	4
A-4	S 3	10.8	13	B-4	U 3	11.0	TUBE	C-4	S 3	10.8	11	D-4	S 3	10.8	24
A-4	S 4	15.8	18	B-4	S 4	15.8	15	C-4	S 4	15.8	14	D-4	S 4	15.8	22
A-4	S 5	20.8	12	B-4	S 5	20.8	21	C-4	S 5	20.8	15	D-4	S 5	20.8	9
A-4	S 6	25.8	20	B-4	S 6	25.8	21	C-4	S 6	25.8	20	D-4	S 6	25.8	16
A-4	S 7	30.8	50	B-4	S 7	30.8	34	C-4	S 7	30.8	21	D-4	S 7	30.8	65
A-4	S 8	35.8	93	B-4	S 8	35.8	41	C-4	S 8	35.8	80	D-4	S 8	35.8	88
				B-4	S 9	40.8	95	C-4	S 9	40.8	150	D-4	S 9	40.8	67
				B-4	S 10	45.8	100	C-4	S 10	45.8	70	D-4	S 10	45.8	83
				B-4	S 11	50.8	135	C-4	S 11	50.8	135/11"	D-4	S 11	50.8	160
												D-4	S 12	55.8	132
												D-4	S 13	60.8	45
												D-4	S 14	65.8	100
												D-4	S 15	70.4	100/3"
												D-4	S 16	75.4	100/2"
												D-4	S 17	80.3	50/0"
												D-4	S 18	85.4	100/3"
												D-4	S 19	90.1	100/4"
												D-4	S 20	95.6	170/9"
												D-4	S 21	100.3	50/0"

TABLE 3

TABLE 1
MATRIX OF SPT BLOW COUNT DATA IN PROPOSED EMPLACEMENT AREA
N < 10 BLOWS/FT FOR ALL SAMPLES

ID	Sample	z _{avg}	N	ID	Sample	z _{avg}	N	ID	Sample	z _{avg}	N	ID	Sample	z _{avg}	N
A-1	S 1	0.8	23	B-1	S 1	0.8	13	C-1	S 1	0.8	3	D-1	S 1	0.8	40
A-1	S 2	5.8	13	B-1	U 2	6.0	TUBE	C-1	S 2	5.8	8	D-1	S 2	5.8	12
A-1	S 3	10.8	22	B-1	S 3	10.8	15	C-1	U 3	11.0	TUBE	D-1	S 3	10.8	14
A-1	S 4	15.8	19	B-1	S 4	15.8	20	C-1	S 4	15.8	16	D-1	S 4	15.8	13
A-1	S 5	20.8	13	B-1	S 5	20.8	12	C-1	S 5	20.8	8	D-1	S 5	20.8	16
A-1	S 6	25.8	36	B-1	S 6	25.8	45	C-1	S 6	25.8	60	D-1	S 6	25.8	100
A-1	S 7	30.8	149	B-1	S 7	30.8	70	C-1	S 7	30.8	91	D-1	S 7	30.8	90
A-1	S 8	35.8	114	B-1	S 8	35.8	90	C-1	S 8	35.8	45	D-1	S 8	35.8	75
A-1	S 9	40.8	70	B-1	S 9	40.8	33	C-1	S 9	40.8	115	D-1	S 9	40.8	100
A-1	S 10	45.8	80	B-1	S 10	45.8	63	C-1	S 10	45.8	85	D-1	S 10	45.8	110
A-1	S 11	50.8	120	B-1	S 11	50.8	125	C-1	S 11	50.8	110	D-1	S 11	50.8	138
A-1	S 12	55.8	110												
A-1	S 13	60.8	102												
A-1	S 14	65.8	54												
A-1	S 15	67.0	100/6"												
A-1	S 16	70.8	100+												
A-1	S 17	75.5	100/6"												
A-1	S 18	80.2	100/4"												
A-1	S 19	85.2	100/4"												
A-1	S 20	90.5	100/6"												
A-1	S 21	95.3	100/6"												
A-1	S 22	100.5	100/6"												

A-2	S 1	0.8	1	B-2	S 1	0.8	4	C-2	S 1	0.8	18	D-2	S 1	0.8	6
A-2	U 2	6.0	TUBE	B-2	S 2	5.8	5	C-2	U 1	6.0	TUBE	D-2	S 2	5.8	6
A-2	S 3	10.8	11	B-2	U 1	9.0	TUBE	C-2	U 2	11.0	TUBE	D-2	S 3	10.8	11
A-2	S 4	15.8	14	B-2	S 3	10.8	13	C-2	S 2	15.8	13	D-2	S 4	15.8	15
A-2	S 5	20.8	17	B-2	S 4	15.8	16	C-2	S 3	20.8	11	D-2	S 5	20.8	18
A-2	S 6	25.8	16	B-2	S 5	20.8	12	C-2	S 4	25.8	34	D-2	S 6	25.8	17
A-2	S 7	30.8	51	B-2	S 6	25.8	15	C-2	S 5	30.8	187/8"	D-2	S 7	30.8	107
A-2	S 8	35.8	175/11"	B-2	S 7	30.8	71	C-2	S 6	35.8	128	D-2	S 8	35.8	121
A-2	S 9	40.8	100/4"	B-2	S 8	35.8	171/11"	C-2	S 7	40.8	181/11"	D-2	S 9	40.8	105
A-2	S 10	45.8	105	B-2	S 9	40.8	68	C-2	S 8	45.8	84	D-2	S 10	45.8	80
A-2	S 11	50.5	100/6"	B-2	S 10	45.8	100/5"	C-2	S 9	50.8	120	D-2	S 11	50.8	150
				B-2	S 11	50.5	100/6"								

A-3	S 1	0.8	4	B-3	S 1	0.8	9	C-3	S 1	0.8	11	D-3	S 1	0.8	6
A-3	S 2	5.8	9	B-3	U 1	6.0	TUBE	C-3	S 2	5.8	6	D-3	S 2	5.8	14
A-3	S 3	10.8	15	B-3	U 2	11.0	TUBE	C-3	S 3	10.8	8	D-3	S 3	10.8	11
A-3	S 4	15.8	15	B-3	S 2	15.8	18	C-3	S 4	15.8	10	D-3	S 4	15.8	9
A-3	S 5	20.8	20	B-3	S 3	20.8	12	C-3	S 5	20.8	9	D-3	S 5	20.8	11
A-3	S 6	25.8	30	B-3	S 4	25.8	24	C-3	S 6	25.8	22	D-3	S 6	25.8	39
A-3	S 7	30.8	34	B-3	S 5	30.8	28	C-3	S 7	30.8	135	D-3	S 7	30.8	100/4"
A-3	S 8	35.8	114	B-3	S 6	35.8	141	C-3	S 8	35.5	100/6"	D-3	S 8	35.3	100/5"
A-3	S 9	40.8	175	B-3	S 7	40.8	150	C-3	S 9	40.8	94	D-3	S 9	40.5	100/5"
A-3	S 10	45.8	82	B-3	S 8	45.8	52	C-3	S 10	45.8	143/11"	D-3	S 10	45.5	100/4"
A-3	S 11	50.5	100/5"	B-3	S 9	50.8	115	C-3	S 11	50.5	100/5"	D-3	S 11	50.8	75/6"

A-4	S 1	0.8	14	B-4	S 1	0.8	22	C-4	S 1	0.8	15	D-4	S 1	0.8	8
A-4	S 2	5.8	18	B-4	S 2	5.8	9	C-4	S 2	5.8	7	D-4	S 2	5.8	4
A-4	S 3	10.8	13	B-4	U 3	11.0	TUBE	C-4	S 3	10.8	11	D-4	S 3	10.8	24
A-4	S 4	15.8	18	B-4	S 4	15.8	15	C-4	S 4	15.8	14	D-4	S 4	15.8	22
A-4	S 5	20.8	12	B-4	S 5	20.8	21	C-4	S 5	20.8	15	D-4	S 5	20.8	9
A-4	S 6	25.8	20	B-4	S 6	25.8	21	C-4	S 6	25.8	20	D-4	S 6	25.8	16
A-4	S 7	30.8	50	B-4	S 7	30.8	34	C-4	S 7	30.8	21	D-4	S 7	30.8	65
A-4	S 8	35.8	93	B-4	S 8	35.8	41	C-4	S 8	35.8	80	D-4	S 8	35.8	88
				B-4	S 9	40.8	95	C-4	S 9	40.8	150	D-4	S 9	40.8	67
				B-4	S 10	45.8	100	C-4	S 10	45.8	70	D-4	S 10	45.8	83
				B-4	S 11	50.8	135	C-4	S 11	50.8	135/11"	D-4	S 11	50.8	160
												D-4	S 12	55.8	132
												D-4	S 13	60.8	45
												D-4	S 14	65.8	100
												D-4	S 15	70.4	100/3"
												D-4	S 16	75.4	100/2"
												D-4	S 17	80.3	50/0"
												D-4	S 18	85.4	100/3"
												D-4	S 19	90.1	100/4"
												D-4	S 20	95.6	170/9"
												D-4	S 21	100.3	50/0"

TABLE 1

9903290209-01

TABLE 2
MATRIX OF SPT BLOW COUNT DATA IN PROPOSED EMPLACEMENT AREA
N < 10 BLOWS/FT BELOW A DEPTH OF 1.5 FT

ID	Sample	z _{avg}	N	ID	Sample	z _{avg}	N	ID	Sample	z _{avg}	N	ID	Sample	z _{avg}	N
A-1	S 2	5.8	13	B-1	U 2	6.0	TUBE	C-1	S 2	5.8	8	D-1	S 2	5.8	12
A-1	S 3	10.8	22	B-1	S 3	10.8	15	C-1	U 3	11.0	TUBE	D-1	S 3	10.8	14
A-1	S 4	15.8	19	B-1	S 4	15.8	20	C-1	S 4	15.8	16	D-1	S 4	15.8	13
A-1	S 5	20.8	13	B-1	S 5	20.8	12	C-1	S 5	20.8	8	D-1	S 5	20.8	16
A-1	S 6	25.8	36	B-1	S 6	25.8	45	C-1	S 6	25.8	60	D-1	S 6	25.8	100
A-1	S 7	30.8	149	B-1	S 7	30.8	70	C-1	S 7	30.8	91	D-1	S 7	30.8	90
A-1	S 8	35.8	114	B-1	S 8	35.8	90	C-1	S 8	35.8	45	D-1	S 8	35.8	75
A-1	S 9	40.8	70	B-1	S 9	40.8	33	C-1	S 9	40.8	115	D-1	S 9	40.8	100
A-1	S 10	45.8	80	B-1	S 10	45.8	63	C-1	S 10	45.8	85	D-1	S 10	45.8	110
A-1	S 11	50.8	120	B-1	S 11	50.8	125	C-1	S 11	50.8	110	D-1	S 11	50.8	138
A-1	S 12	55.8	110												
A-1	S 13	60.8	102												
A-1	S 14	65.8	54												
A-1	S 15	67.0	100/6"												
A-1	S 16	70.8	100+												
A-1	S 17	75.5	100/6"												
A-1	S 18	80.2	100/4"												
A-1	S 19	85.2	100/4"												
A-1	S 20	90.5	100/6"												
A-1	S 21	95.3	100/6"												
A-1	S 22	100.5	100/6"												

A-2	U 2	6.0	TUBE	B-2	S 2	5.8	5	C-2	U 1	6.0	TUBE	D-2	S 2	5.8	6
A-2	S 3	10.8	11	B-2	U 1	9.0	TUBE	C-2	U 2	11.0	TUBE	D-2	S 3	10.8	11
A-2	S 4	15.8	14	B-2	S 3	10.8	13	C-2	S 2	15.8	13	D-2	S 4	15.8	15
A-2	S 5	20.8	17	B-2	S 4	15.8	16	C-2	S 3	20.8	11	D-2	S 5	20.8	18
A-2	S 6	25.8	16	B-2	S 5	20.8	12	C-2	S 4	25.8	34	D-2	S 6	25.8	17
A-2	S 7	30.8	51	B-2	S 6	25.8	15	C-2	S 5	30.8	187/8"	D-2	S 7	30.8	107
A-2	S 8	35.8	175/11"	B-2	S 7	30.8	71	C-2	S 6	35.8	128	D-2	S 8	35.8	121
A-2	S 9	40.4	100/4"	B-2	S 8	35.8	171/11"	C-2	S 7	40.8	181/11"	D-2	S 9	40.8	105
A-2	S 10	45.8	105	B-2	S 9	40.8	68	C-2	S 8	45.8	84	D-2	S 10	45.8	80
A-2	S 11	50.5	100/6"	B-2	S 10	45.8	100/5"	C-2	S 9	50.8	120	D-2	S 11	50.8	150
				B-2	S 11	50.5	100/6"								

A-3	S 2	5.8	9	B-3	U 1	6.0	TUBE	C-3	S 2	5.8	6	D-3	S 2	5.8	14
A-3	S 3	10.8	15	B-3	U 2	11.0	TUBE	C-3	S 3	10.8	8	D-3	S 3	10.8	11
A-3	S 4	15.8	15	B-3	S 2	15.8	18	C-3	S 4	15.8	10	D-3	S 4	15.8	9
A-3	S 5	20.8	20	B-3	S 3	20.8	12	C-3	S 5	20.8	9	D-3	S 5	20.8	11
A-3	S 6	25.8	30	B-3	S 4	25.8	24	C-3	S 6	25.8	22	D-3	S 6	25.8	39
A-3	S 7	30.8	34	B-3	S 5	30.8	28	C-3	S 7	30.8	135	D-3	S 7	30.8	100/4"
A-3	S 8	35.8	114	B-3	S 6	35.8	141	C-3	S 8	35.5	100/6"	D-3	S 8	35.3	100/5"
A-3	S 9	40.8	175	B-3	S 7	40.8	150	C-3	S 9	40.8	94	D-3	S 9	40.5	100/5"
A-3	S 10	45.8	82	B-3	S 8	45.8	52	C-3	S 10	45.8	143/11"	D-3	S 10	45.5	100/4"
A-3	S 11	50.5	100/5"	B-3	S 9	50.8	115	C-3	S 11	50.5	100/5"	D-3	S 11	50.8	75/6"

A-4	S 2	5.8	18	B-4	S 2	5.8	9	C-4	S 2	5.8	7	D-4	S 2	5.8	4
A-4	S 3	10.8	13	B-4	U 3	11.0	TUBE	C-4	S 3	10.8	11	D-4	S 3	10.8	24
A-4	S 4	15.8	18	B-4	S 4	15.8	15	C-4	S 4	15.8	14	D-4	S 4	15.8	22
A-4	S 5	20.8	12	B-4	S 5	20.8	21	C-4	S 5	20.8	15	D-4	S 5	20.8	9
A-4	S 6	25.8	20	B-4	S 6	25.8	21	C-4	S 6	25.8	20	D-4	S 6	25.8	16
A-4	S 7	30.8	50	B-4	S 7	30.8	34	C-4	S 7	30.8	21	D-4	S 7	30.8	65
A-4	S 8	35.8	93	B-4	S 8	35.8	41	C-4	S 8	35.8	80	D-4	S 8	35.8	88
				B-4	S 9	40.8	95	C-4	S 9	40.8	150	D-4	S 9	40.8	67
				B-4	S 10	45.8	100	C-4	S 10	45.8	70	D-4	S 10	45.8	83
				B-4	S 11	50.8	135	C-4	S 11	50.8	135/11"	D-4	S 11	50.8	160
												D-4	S 12	55.8	132
												D-4	S 13	60.8	45
												D-4	S 14	65.8	100
												D-4	S 15	70.4	100/3"
												D-4	S 16	75.4	100/2"
												D-4	S 17	80.3	50/0"
												D-4	S 18	85.4	100/3"
												D-4	S 19	90.1	100/4"
												D-4	S 20	95.6	170/9"
												D-4	S 21	100.3	50/0"

APL 10-11-99
C-4
Also available on
Aperture

TABLE 2

9903290209-02

TABLE 3
MATRIX OF SPT BLOW COUNT DATA IN PROPOSED EMPLACEMENT AREA
10 < N < 15 BLOWS/FT BELOW A DEPTH OF 1.5 FEET

ID	Sample	z _{avg}	N	ID	Sample	z _{avg}	N	ID	Sample	z _{avg}	N	ID	Sample	z _{avg}	N
A-1	S 2	5.8	13	B-1	U 2	6.0	TUBE	C-1	S 2	5.8	8	D-1	S 2	5.8	12
A-1	S 3	10.8	22	B-1	S 3	10.8	15	C-1	U 3	11.0	TUBE	D-1	S 3	10.8	14
A-1	S 4	15.8	19	B-1	S 4	15.8	20	C-1	S 4	15.8	16	D-1	S 4	15.8	13
A-1	S 5	20.8	13	B-1	S 5	20.8	12	C-1	S 5	20.8	8	D-1	S 5	20.8	16
A-1	S 6	25.8	36	B-1	S 6	25.8	45	C-1	S 6	25.8	60	D-1	S 6	25.8	100
A-1	S 7	30.8	149	B-1	S 7	30.8	70	C-1	S 7	30.8	91	D-1	S 7	30.8	90
A-1	S 8	35.8	114	B-1	S 8	35.8	90	C-1	S 8	35.8	45	D-1	S 8	35.8	75
A-1	S 9	40.8	70	B-1	S 9	40.8	33	C-1	S 9	40.8	115	D-1	S 9	40.8	100
A-1	S 10	45.8	80	B-1	S 10	45.8	63	C-1	S 10	45.8	85	D-1	S 10	45.8	110
A-1	S 11	50.8	120	B-1	S 11	50.8	125	C-1	S 11	50.8	110	D-1	S 11	50.8	138
A-1	S 12	55.8	110												
A-1	S 13	60.8	102												
A-1	S 14	65.8	54												
A-1	S 15	67.0	100/6"												
A-1	S 16	70.8	100+												
A-1	S 17	75.5	100/6"												
A-1	S 18	80.2	100/4"												
A-1	S 19	85.2	100/4"												
A-1	S 20	90.5	100/6"												
A-1	S 21	95.3	100/6"												
A-1	S 22	100.5	100/6"												

A-2	U 2	6.0	TUBE	B-2	S 2	5.8	5	C-2	U 1	6.0	TUBE	D-2	S 2	5.8	6
A-2	S 3	10.8	11	B-2	U 1	9.0	TUBE	C-2	U 2	11.0	TUBE	D-2	S 3	10.8	11
A-2	S 4	15.8	14	B-2	S 3	10.8	13	C-2	S 2	15.8	13	D-2	S 4	15.8	15
A-2	S 5	20.8	17	B-2	S 4	15.8	16	C-2	S 3	20.8	11	D-2	S 5	20.8	18
A-2	S 6	25.8	16	B-2	S 5	20.8	12	C-2	S 4	25.8	34	D-2	S 6	25.8	17
A-2	S 7	30.8	51	B-2	S 6	25.8	15	C-2	S 5	30.8	187/8"	D-2	S 7	30.8	107
A-2	S 8	35.8	175/11"	B-2	S 7	30.8	71	C-2	S 6	35.8	128	D-2	S 8	35.8	121
A-2	S 9	40.4	100/4"	B-2	S 8	35.8	171/11"	C-2	S 7	40.8	181/11"	D-2	S 9	40.8	105
A-2	S 10	45.8	105	B-2	S 9	40.8	68	C-2	S 8	45.8	84	D-2	S 10	45.8	80
A-2	S 11	50.5	100/6"	B-2	S 10	45.8	100/5"	C-2	S 9	50.8	120	D-2	S 11	50.8	150
				B-2	S 11	50.5	100/6"								

A-3	S 2	5.8	9	B-3	U 1	6.0	TUBE	C-3	S 2	5.8	6	D-3	S 2	5.8	14
A-3	S 3	10.8	15	B-3	U 2	11.0	TUBE	C-3	S 3	10.8	8	D-3	S 3	10.8	11
A-3	S 4	15.8	15	B-3	S 2	15.8	18	C-3	S 4	15.8	10	D-3	S 4	15.8	9
A-3	S 5	20.8	20	B-3	S 3	20.8	32	C-3	S 5	20.8	9	D-3	S 5	20.8	11
A-3	S 6	25.8	30	B-3	S 4	25.8	24	C-3	S 6	25.8	22	D-3	S 6	25.8	39
A-3	S 7	30.8	34	B-3	S 5	30.8	28	C-3	S 7	30.8	135	D-3	S 7	30.8	100/4"
A-3	S 8	35.8	114	B-3	S 6	35.8	141	C-3	S 8	35.5	100/6"	D-3	S 8	35.3	100/5"
A-3	S 9	40.8	175	B-3	S 7	40.8	150	C-3	S 9	40.8	94	D-3	S 9	40.5	100/5"
A-3	S 10	45.8	82	B-3	S 8	45.8	52	C-3	S 10	45.8	143/11"	D-3	S 10	45.5	100/4"
A-3	S 11	50.5	100/5"	B-3	S 9	50.8	115	C-3	S 11	50.5	100/5"	D-3	S 11	50.8	75/6"

A-4	S 2	5.8	18	B-4	S 2	5.8	9	C-4	S 2	5.8	7	D-4	S 2	5.8	4
A-4	S 3	10.8	13	B-4	U 3	11.0	TUBE	C-4	S 3	10.8	11	D-4	S 3	10.8	24
A-4	S 4	15.8	18	B-4	S 4	15.8	15	C-4	S 4	15.8	14	D-4	S 4	15.8	22
A-4	S 5	20.8	12	B-4	S 5	20.8	21	C-4	S 5	20.8	15	D-4	S 5	20.8	9
A-4	S 6	25.8	20	B-4	S 6	25.8	21	C-4	S 6	25.8	20	D-4	S 6	25.8	16
A-4	S 7	30.8	50	B-4	S 7	30.8	34	C-4	S 7	30.8	21	D-4	S 7	30.8	65
A-4	S 8	35.8	93	B-4	S 8	35.8	41	C-4	S 8	35.8	80	D-4	S 8	35.8	88
				B-4	S 9	40.8	95	C-4	S 9	40.8	150	D-4	S 9	40.8	67
				B-4	S 10	45.8	100	C-4	S 10	45.8	70	D-4	S 10	45.8	83
				B-4	S 11	50.8	135	C-4	S 11	50.8	135/11"	D-4	S 11	50.8	160
												D-4	S 12	55.8	132
												D-4	S 13	60.8	45
												D-4	S 14	65.8	100
												D-4	S 15	70.4	100/3"
												D-4	S 16	75.4	100/2"
												D-4	S 17	80.3	50/0"
												D-4	S 18	85.4	100/3"
												D-4	S 19	90.1	100/4"
												D-4	S 20	95.6	170/9"
												D-4	S 21	100.3	50/0"

AP-570
C-4
Also see
AP-570

TABLE 3

9903290209-03